Hindawi Publishing Corporation
ISRN Astronomy and Astrophysics
Volume 2014, Article ID 843169, 1 page
http://dx.doi.org/10.1155/2014/843169

Retraction

Retracted: On the Geoeffectiveness Structure of Solar Wind-Magnetosphere Coupling Functions during Intense Storms

ISRN Astronomy and Astrophysics

Received 18 December 2013; Accepted 18 December 2013; Published 23 January 2014

The article titled "On the Geoeffectiveness Structure of Solar Wind-Magnetosphere Coupling Functions during Intense Storms" [1], published in ISRN Astronomy and Astrophysics, has been retracted as it is found to contain a substantial amount of material from the article by Yermolaev, Y. I., and M. Y. Yermolaev (2008), Comment on "Interplanetary origin of intense geomagnetic storms ($Dst < -100$ nT) during solar cycle 23" by W. D. Gonzalez et al. Geophys. Res. Lett., 35, L01101, doi:10.1029/2007GL030281.

References

[1] B. Olufemi Adebesin, S. Oluwole Ikubanni, and J. Stephen Kayode, "On the geoeffectiveness structure of solar wind-magnetosphere coupling functions during intense storms," *ISRN Astronomy and Astrophysics*, vol. 2011, Article ID 961757, 13 pages, 2011.

International Scholarly Research Network
ISRN Astronomy and Astrophysics
Volume 2011, Article ID 961757, 13 pages
doi:10.5402/2011/961757

Research Article

On the Geoeffectiveness Structure of Solar Wind-Magnetosphere Coupling Functions during Intense Storms

B. Olufemi Adebesin, S. Oluwole Ikubanni, and J. Stephen Kayode

Space Weather Research Group, Department of Industrial Physics, College of Science & Engineering, Landmark University, PMB 1001, Omu Aran, Kwara State, Nigeria

Correspondence should be addressed to B. Olufemi Adebesin, f_adebesin@yahoo.co.uk

Received 28 September 2011; Accepted 10 November 2011

Academic Editors: G. Chernov and M. Ding

The geoeffectiveness of some coupling functions for the Solar Wind-Magnetosphere Interaction had been studied. 58 storms with peak Dst < -100 nT were used. The result showed that the interplanetary magnetic field B_z appeared to be more relevant with the magnetic field B (which agreed with previous results). However, both the V (solar wind flow speed) and B_z factors in the interplanetary dawn-dusk electric field ($V \times B_z$) are effective in the generation of very intense storms (peak Dst < -250 nT) while "intense" storms (-250 nT $\leq$ peak Dst < -100 nT) are mostly enhanced by the B_z factor alone (in most cases). The southward B_z duration B_T seems to be more relevant for Dst < -250 nT class of storms and invariably determines the recovery phase duration. Most of the storms were observed to occur at midnight hours (i.e., 2100–0400 UT), having a 41.2% incidence rate, with high frequency between 2300 UT and 0000 UT. 62% of the events were generated as a result of Magnetic Cloud (MC), while 38% were generated by complex ejecta. The B-B_z relation for the magnetic cloud attained a correlation coefficient of 0.8922, while it is 0.7608 for the latter. Conclusively, B_z appears to be the most geoeffective factor, and geoeffectiveness should be a factor that depends on methods of event identification and classification as well as the direction of event correlation.

1. Introduction

Magnetic storm occurs at periods during which the global magnetic field, as measured by low-latitude ground magnetometers, significantly decreases. The intensity of the storm is characterized by the minimum peak Dst index [1], such that during intense storms the global field decreases at least a hundred nT (out of about 30,000 nT ground field at the equator). The interplanetary causes of such long-duration global magnetic field disturbances have been related to an intense and long-lasting southward IMF associated with the duskward interplanetary electric field (IEF) that is the main driver of global convection in the magnetosphere. For instance, Gonzalez and Tsurutani [2] define a southward IMF of at least -10 nT for more than 3 hours as a sufficient condition for the development of an intense magnetic storm. They further associate these long-duration and intense IEF enhancements either with high-speed streams or with solar wind density enhancement events, presumably known as coronal mass ejections (CMEs). These are large plasma clouds ejected from the Sun and which are characterized by intense flux-rope-like magnetic fields and low dynamic pressures. As the CMEs often travel faster than the ambient solar wind, a shock front develops in front of the CME. The interplanetary manifestation of a CME is called an interplanetary CME (ICME). However, Gosling et al. [3] had suggested that CMEs, particularly those associated with a shock, are regarded as the most important drivers of strong global geomagnetic activity.

According to Lu et al. [4], the interaction between the solar wind and the Earth's magnetosphere produces a system of plasma circulation in the magnetosphere and high latitude ionosphere. The ionospheric convection configuration therefore provides important information of the solar wind-magnetosphere coupling. However, to predict the occurrence of a magnetic storm, according to Gonzalez et al. [5], one needs to be able to predict three interplanetary parameters: southward turning B_z, flow speed V, and the southward

duration of B_z (i.e., B_T). Moreover, Gonzalez et al. [1] gave a summary of some of the most commonly used coupling functions for the Solar Wind-Magnetosphere Interaction amongst which are $V \times B_z$ [6, 7], B_z [8, 9], $B_z V^2$ [10], and $B_z^2 V$ [11].

In the work of Adebesin [12], while studying the probable roles of interplanetary and geomagnetic parameters in the generation of "intense" and "very intense" magnetic storms as well as the correlation between magnetic field intensity B with flow speed V, southward turning of B_z (B_s), and B_s duration B_T, a total of 18 storm events were observed (8 intense storms ($-250\,\text{nT} \leq$ peak Dst $< -100\,\text{nT}$) and 10 "very intense" (peak Dst $< -250\,\text{nT}$) ones), from where it was observed that generally for the storms, the flow speed is the most correlated and hence the most geoeffective. These agree in part with the results of Gosling et al. [3] and Taylor et al. [13], who have shown statistically that out of all the variety of ejecta fields, the ones that are most effective in creating magnetic storms are events that are fast, with speeds exceeding the ambient wind speed by the magnetosonic wave speed, thereby causing a fast forward shock, The result of Adebesin [12] further showed that "very intense" storms present a negligible correlation between the flow speed and the magnetic field intensity B whereas "intense" storms have 0.587 correlation between the two parameters. The present work is presented to ascertain whether the result would follow the same pattern for larger database of magnetic activities, as well as the validation of other "indicators" used in the coupling functions for the Solar Wind-Magnetosphere Interaction, as mentioned in the second paragraph. The choice of the magnetic field intensity is because for fast ICMEs, the solar ejecta and their upstream sheaths (behind the shocks) contain intense magnetic fields giving them a statistically higher probability of the right conditions to generate magnetic storms [14].

The choice of solar wind flow speed V, southward turning of B_z, and B_z duration (B_T) could also be attributed to their roles in previous works. For instance, from the work of Dal Lago et al. ([15], and references therein), 5 great geomagnetic storms with Dst $< -250\,\text{nT}$, observed in the period of 1978-1979, were studied, and it was found that two types of interplanetary cause were present. First was the shock compressed magnetic field, and the other was the magnetic cloud field. The first is due to a shock wave propagating in the solar wind, probably driven by a CME-related structure (ejecta), which compresses the existing solar wind magnetic field, that by chance can be pointing antiparallel to the Earth's magnetic field (i.e., negative B_z direction), and the second believed to be the ejected material from the CMEs, similar to interplanetary magnetic clouds. Ballatore [16] however observed that high solar wind speeds the processes responsible for the energy transfer between the interplanetary medium and the magnetosphere saturate. In addition, the influence of internal magnetospheric plasma physics on the geomagnetic activity may be larger for the faster solar wind intervals and concluded that an order in the interplanetary-magnetosphere coupling is significant only until a certain threshold of solar wind speed ($\sim$550 km/s).

Table 1: Classification of magnetic storms on the basis of the Dst index using the 1957–1993 measurements (after [17]).

Class	Number	%	Dst range (nT)
Weak	482	44	−30–−50
Moderate	346	32	−50–−100
Strong (i.e., intense)	206	19	−100–−200
Severe (very-intense)	45	4	−200–−350
Great	6	1	< -350

Dal Lago et al. [15] also studied the solar and interplanetary causes of the 9 great geomagnetic storms (Dst $< -200\,\text{nT}$) observed from January 1997 to April 2001 and found out that the sources of the interplanetary southward magnetic field B_s, responsible for the occurrence of the storms, were related to either (i) the intensified shock/sheath field, (ii) interplanetary magnetic clouds field, or (iii) the combination of sheath-cloud or sheath-ejecta field. One of the events was related to a slow CME, with CME expansion speed not greater than 550 km/s. Gonzalez et al. ([5], and references therein), in an analysis of more than 1200 magnetic storms, showed that double/triple-step storms are caused by two IMF southward field events of approximately equal strength. However, a likely explanation is that the first event was caused by sheath southward IMFs (shocked, slow solar wind plasma and fields) and the second was from the remnants of the ICME itself (magnetic cloud). However, a plot of peak values of magnetic field intensity B (nT) and the solar wind speed for the magnetic cloud events shows that the faster the cloud moves, the higher is the core magnetic field.

Huang et al. [18] in their studies of the magnetic storm of October 29–31, 2003, often referred to as the Halloween storm, reported that the storm is characterized by extremely high solar wind speeds and three southward IMF turnings within the interval. Moreover, Vieira et al. [19] have shown that about 15% of intense storms caused by magnetic clouds can be of the triple-step type, especially when large amplitude density waves/discontinuities exist within the cloud, thus causing an additional Bs structure.

2. Data and Methods

In the present study, a total of 58 storm events were presented. 40 of the storms were intense (i.e., $-250\,\text{nT} \leq$ peak Dst $< -100\,\text{nT}$) and the remaining 18 were "very intense" or severe (i.e., peak Dst $< -250\,\text{nT}$). It should be noted that very intense storms are not so common, hence the reason for the limited number of events when compared to the intense ones. For instance, no intense geomagnetic activity was recorded between December 18, 2006 and July 2011. The one that occurred on August 8, 2011 does not have the required parameters for this study. Moreover, Table 1 also supported the argument that very-intense storms are not so common like the other ones. The table highlighted the basic classification of magnetic storms on the basis of the Dst index using the 1957–1993 measurements (according to [17]). It was shown that very-intense (i.e., Severe and Great) storms

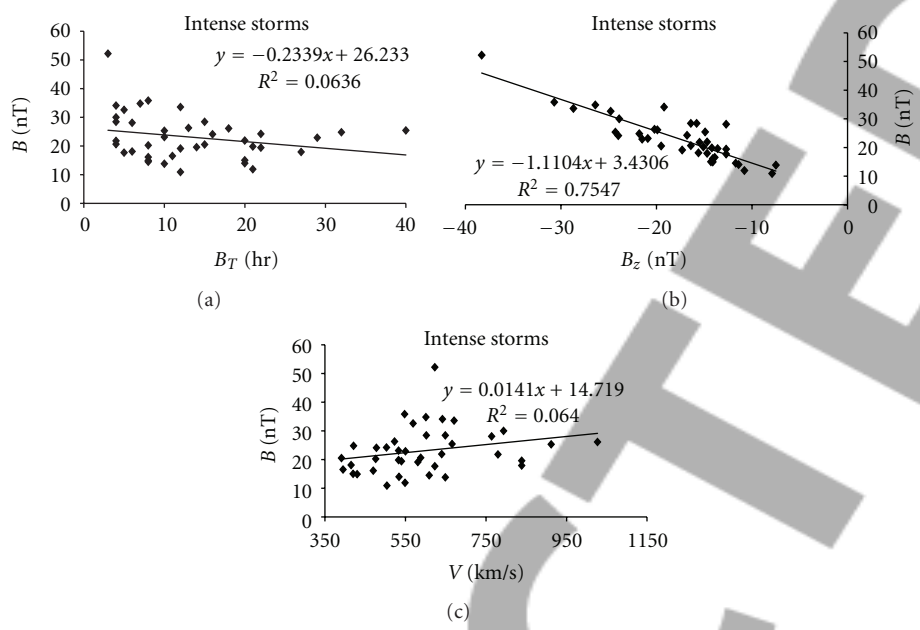

Figure 1: Regression plots of (a) B versus B_T, (b) B versus B_z, and (c) B versus V for intense storms.

take just about 5% of the list. Weak (44%), moderate (32%), and strong (i.e., intense) storms take 19%.

The authors decided to divide the storms into these 2 categories (i.e., "intense" and "very-intense") so as to be able to understand the storms behavior at peak Dst < -250 nT, and not just generally at -250 nT $\leq$ peak Dst < -100 nT condition alone. The NSSDC's OMNI database (http://nssdc.gsfc.nasa.gov/omniweb/) provided the hourly values of the low latitude magnetic index Dst (nT), the solar wind flow speed V (km/s), the imbedded magnetic field intensity B (nT), and the southward Interplanetary magnetic field B_z (nT)—in GSM. B_T was thereafter calculated from B_z. Presented in Tables 2 and 3, respectively, are the lists of storm dates with corresponding peak values of Dst, magnetic field intensity B, IMF B_z, B_z southward turning interval B_T, and solar wind flow speed V, within the storm interval, as well as the calculated values for some coupling functions for the Solar Wind-Magnetosphere Interaction for "intense" and "very intense" conditions. The hourly peak values of B, B_z, and V taken are generally near Dst hourly maximum depression. The only exception to this condition is the event of 13 March 1989 (in which the Cliver values were used, i.e., $V \approx 550$ km/s). It is assumed that the intensity of the storm makes the measurement of the other parameters to be impossible at Dst maximum depression.

All the B, B_z, and V values are approximate with a possible uncertainty of ~5%. This is because the respective peak values of the three parameters may differ from their values at Dst maximum depression by around 5% or less. Thereafter, the Regression fit was plotted and the correlation coefficients were computed.

3. Results

Figures 1, 2, and 3 present the Regression plots of (a) B versus B_T, (b) B versus B_z, and (c) B versus V for intense, very intense, and all storms, respectively. However, the generated corresponding correlation coefficients for these plots were highlighted in Table 4. From the table, B versus B_z ratio recorded the highest correlation coefficient of 0.868, 0.819, and 0.885 for intense, very-intense, and all storms, respectively. The correlation between the magnetic field intensity B and the flow speed V is low (0.252) for intense storms, 0.439 for very-intense, and 0.489 for all storms. Moreover, B versus B_T (i.e., the southward B_z duration) is rather low for both intense and all storms (~0.250), while it is 0.474 for very-intense ones.

Furthermore, highlighted in Figures 4, 5, and 6 are the regression plots of B with some commonly used coupling functions for the Solar Wind-Magnetosphere Interaction for intense, very-intense, and all storms, respectively: (a) VB_T (b) B_zV^2, (c) $V \times B_z$, (d) $B_{z^2}V$. Table 5 however presents the correlation coefficient between B_zV^2, $B_z \times V$, and $B_{z^2}V$ (according to [1]) as well as the self-derived VB_T,$B_{z^3}V$, and $(V \times B_z)/B_T$ with magnetic field intensity B. Observe from the table that for all the storms, B versus $V \times B_z$ recorded the highest correlation (0.857), followed by $B_{z^2}V$, $B_{z^3}V$, B_zV^2, and $(V \times B_z)/B_T$, in that order (all above 75% range). Note that the B-VB_T relationship is negligible (i.e., 0.085). The $(V \times B_z)/B_T$ ratio is introduced as a function connecting the three parameters used, and it could be seen as yielding good result with B (i.e., 0.750). Moreover, the $B_{z^3}V$ factor used also yielded good correlation strength. However, increasing the power of B_z any further (i.e., $B_{z^n}V$, $n = 4, 5, 6, \ldots$) reduces the B-$B_{z^n}V$ value.

4. Discussion

On the average, B_z had the highest correlation percentage with B, irrespective of whether the storm is intense or very-intense (i.e., above 80%), but as long as the peak Dst ≤ -100 nT condition is satisfied. For the flow speed V,

Table 2: List of intense storm dates with corresponding peak values of average magnetic field B, IMF B_z (GSM), B_z southward turning interval B_T, and solar wind flow speed V, within the storm interval as well as the calculated values for some coupling functions for the Solar Wind-Magnetosphere Interaction.

Storm data	Peak Dst {nT}	Peak B {nT}	Peak B_z {nT}	B_T value {hr}	Peak V {km/s}	Time {UT}	VB_T	$V \times B_z$ {mV/m}	B_zV^2 (exp3)	$B_{z^2}V$ (exp3)	$(V \times B_z)/B_T$	$B_{z^3}V$ (exp4)
Oct. 22, 1999	−237	35.8	−30.7	8.0	548	6.00	4384	16.82	9219	516	2.10	1586
Aug. 12, 2000	−235	33.6	−28.7	12.0	671	9.00	8052	19.26	12922	553	1.60	1586
Aug. 28, 1978	−226	24.1	−24.0	16.0	478	9.00	7648	11.47	5484	275	0.72	661
Sept. 29, 1978	−224	25.3	−24.3	10.0	912	10.00	9120	22.16	20211	539	2.22	1309
June. 5, 1991	−223	32.6	−24.8	5.0	569	19.00	2845	14.11	8029	350	2.82	868
Aug. 24, 2005	−216	52.2	−38.3	3.0	623	11.00	1869	23.86	14865	914	7.95	3500
Sept. 25, 1998	−207	19.6	−13.6	14.0	839	9.00	11746	11.41	9573	155	0.82	211
Apr. 3, 1979	−202	19.1	−17.3	12.0	581	3.00	6972	10.05	5840	174	0.84	301
Sept. 17, 2000	−201	30.0	−23.9	4.0	794	23.00	3176	18.98	15067	454	4.74	1084
Jul. 27, 2004	−197	26.1	−19.9	18.0	1027	13.00	18486	20.44	20989	407	1.14	809
Oct. 21-22, 2001	−187	28.4	−16.4	15.0	649	21.00	9735	10.64	6908	175	0.71	286
Oct. 5, 2000	−182	26.3	−20.2	13.0	523	13.00	6799	10.56	5525	213	0.81	431
Sept. 8, 2002	−181	22.9	−21.5	29.0	550	0.00	15950	11.83	6504	254	0.41	547
Aug. 17, 1970	−181	34.8	−26.4	7.0	601	8.00	4207	15.87	9536	419	2.27	1106
Sept. 30 2002	−176	24.8	−21.8	32.0	421	16.00	13472	9.18	3864	200	0.29	436
Sept. 22, 1999	−173	28.4	−15.8	4.0	602	23.00	2408	9.51	5726	150	2.38	237
Oct. 1, 2001	−166	23.1	−20.9	10.0	533	14.00	5330	11.14	5937	233	1.11	487
Nov. 6, 2000	−159	14.5	−11.7	8.0	609	21.00	4872	7.13	4339	83	0.89	98
Sept. 18, 1979	−158	18.1	−15.6	6.0	415	15.00	2490	6.47	2687	101	1.08	158
Jan. 10, 1976	−156	20.5	−19.5	15.0	391	23.00	5865	7.62	2981	149	0.51	290
Apr. 20, 2002	−149	21.9	−14.7	20.0	640	18.00	12800	9.41	6021	138	0.47	203
Jan. 22, 2004	−149	25.4	−14.9	40.0	666	13.00	26640	9.92	6609	148	0.25	220
Sept. 30, 2001	−148	19.4	−12.7	22.0	540	8.00	11880	6.86	3703	87	0.31	111

Table 2: Continued.

Storm data	Peak Dst {nT}	Peak B {nT}	Peak B_z {nT}	B_T value {hr}	Peak V {km/s}	Time {UT}	VB_T	$V \times B_z$ {mV/m}	$B_z V^2$ (exp3)	$B_{z^2} V$ (exp3)	$(V \times B_z)/B_T$	$B_{z^3} V$ (exp4)
May. 24, 2000	−147	34.1	−19.2	4.0	642	8.00	2568	12.33	7914	237	3.08	454
Dec.15, 2006	−146	17.9	−14.7	27.0	839	7.00	22653	12.33	10348	181	0.46	267
May. 29, 2003	−144	28.1	−12.7	6.0	764	23.00	4584	9.70	7413	123	1.62	156
Mar. 10, 1979	−140	16.1	−14.1	8.0	470	23.00	3760	6.63	3115	93	0.83	132
Mar. 20-21, 1990	−136	17.7	−12.7	5.0	623	6.00	3115	7.91	4929	100	1.58	128
Feb. 12, 2000	−133	20.6	−16.4	4.0	588	11.00	2352	9.64	5670	158	2.41	259
Feb. 16, 1980	−132	14.9	−14.1	8.0	430	7.00	3440	6.06	2607	85	0.76	121
Mar. 29, 1979	−129	11.9	−10.8	21.0	549	21.00	11529	5.93	3255	64	0.28	69
Aug. 30, 2004	−126	15.0	−14.3	20.0	420	22.00	8400	6.01	2523	86	0.30	123
May. 25, 1980	−126	20.2	−15.1	8.0	476	13.00	3808	7.19	3421	109	0.90	164
Jan. 18, 2005	−121	21.8	−15.5	4.0	780	8.00	3120	12.09	9430	187	3.02	290
Apr. 3, 2004	−112	10.9	−7.9	12.0	504	0.00	6048	3.98	2007	31	0.33	25
Apr. 15, 2006	−111	19.8	−14.2	21.0	533	9.00	11193	7.57	4034	107	0.36	153
Feb. 11, 2004	−109	16.5	−13.9	11.0	395	17.00	4345	5.49	2169	76	0.50	106
June. 13, 2005	−106	24.2	−16.8	22.0	503	0.00	11066	8.45	4251	142	0.38	239
Mar. 28, 1984	−105	13.8	−7.5	10.0	649	21.00	6490	4.87	3159	37	0.49	27
Oct. 11, 1980	−104	14.0	−11.4	20.0	534	8.00	10680	6.09	3251	69	0.30	79

Table 3: List of very intense storm dates with every other parameter as in Table 1.

Storm data	Peak Dst {nT}	Peak B {nT}	Peak B_z {nT}	B_T value {hr}	Peak V {km/s}	Time {UT}	VB_T	$V \times B_z$ {mV/m}	$B_z V^2$ (exp3)	$B_{z^2} V$ (exp3)	$(V \times B_z)/B_T$	$B_{z^3} V$ (exp4)
Mar. 13-14, 1989	−589	*20.0	−16.9	—	550	1.00	—	9.30	5112	157	—	265
Nov. 20, 2003	−422	55.8	−50.9	12.0	703	20.00	8436	35.78	25155	1821	2.98	9271
Mar. 31, 2001	−387	47.1	−44.7	5.0	716	8.00	3580	32.01	22916	1431	6.40	6395
May. 26,1967	−387	N/A	—	—	672	4.00	—	—	—	—	—	—
Oct. 30, 2003	−383	38.0	−27.1	12.0	1084	22.00	13008	29.38	31844	796	2.45	2157
Nov. 8, 2004	−373	47.8	−44.9	15.0	730	6.00	10950	32.78	23927	1472	2.19	6608
Nov. 8, 1991	−354	37.4	−9.2	—	482	1.00	—	4.43	2137	41	—	38
Jul. 14, 1982	−325	44.8	−32.3	8.0	947	1.00	7576	30.59	28967	988	3.82	3191
Apr. 13, 1981	−311	31.4	−26.3	11.0	669	6.00	7359	17.59	11771	463	1.60	1217
Feb. 9, 1986	−307	25.1	−17.5	—	856	0.00	—	14.98	12823	262	—	459
Jul. 15, 2000	−301	51.9	−49.4	8.0	1089	0.00	8712	53.80	58584	2658	6.72	13128
Apr. 6-7, 2000	−288	31.4	−27.3	8.0	589	0.00	4712	16.08	9471	439	2.01	1198
Apr. 9, 1990	−281	28.0	−26.6	15.0	484	18.00	7260	12.87	6231	342	0.86	911
Apr. 11, 2001	−271	34.5	−20.5	19.0	732	23.00	13908	15.01	10984	308	0.79	631
Oct. 20, 1989	−268	33.6	−19.4	25.0	918	16.00	22950	17.81	16349	345	0.71	670
Nov. 17, 1989	−266	36.4	−28.0	—	—	22.00	—	—	—	—	—	—
May. 15, 2005	−263	54.2	−38.0	3.0	959	8.00	2877	36.44	34948	1385	12.15	5262
Dec. 19, 1980	−250	37.4	−32.3	9.0	550	18.00	4950	17.77	9771	574	1.97	1853

* Data was not available at that particular hour because of the severeness of the storm, the value used is the first closest observed datum for the peak B.

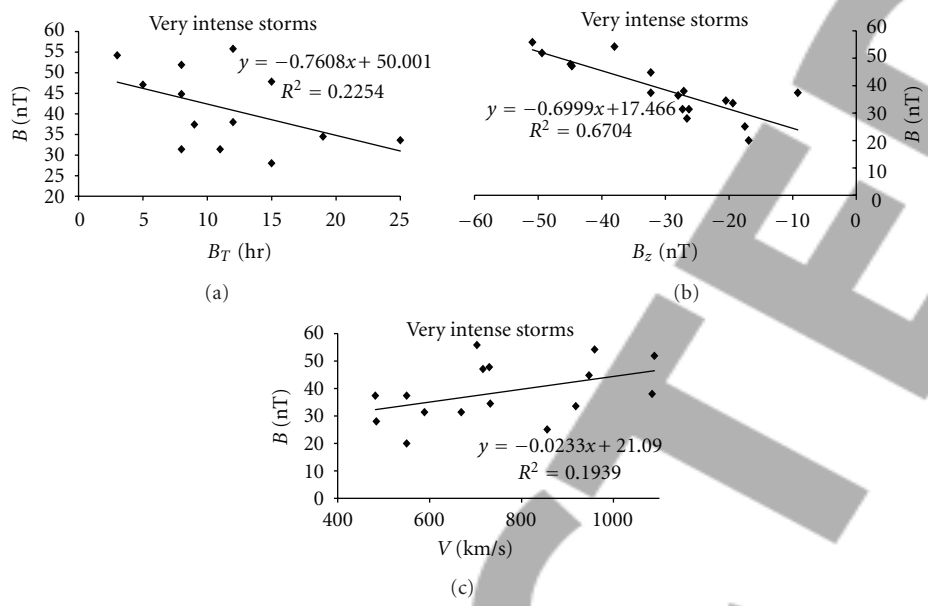

Figure 2: Regression plots of (a) B versus B_T, (b) B versus B_z, and (c) B versus V for very intense storms.

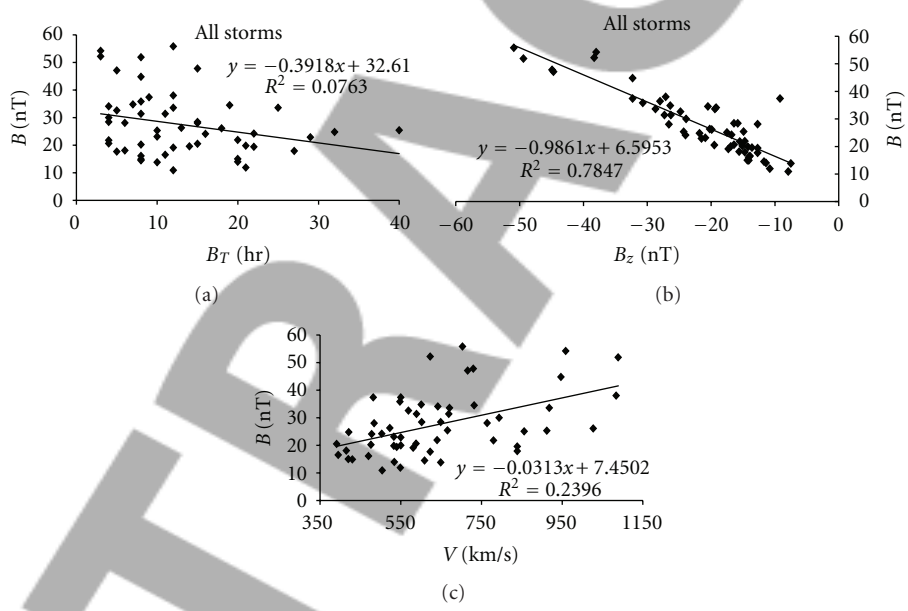

Figure 3: Regression plots of (a) B versus B_T, (b) B versus B_z, and (c) B versus V for all storms.

Table 4: Pearson correlation coefficient between B_T, B_z, and V with average magnetic field B.

Nature	B versus V	B versus B_z	B versus B_T
Intense	0.252	0.868	0.251
Very intense	0.439	0.819	0.474
All	0.489	0.885	0.276

the correlation is approximately 49% for all the 58 storms considered, but rather too low for intense storms alone. The southward B_z duration's (B_T) correlation is very weak in all, but a little below average (47%) for very-intense storms. It follows therefore from these results that the interplanetary dawn dusk electric field, given by $V \times B_z$, is enhanced only by B_z for intense (i.e., $-250\,\text{nT} \leq$ peak Dst $< -100\,\text{nT}$) and by both factors (V and B_z) for "very intense" (i.e., peak Dst $\leq -250\,\text{nT}$) storms. The latter statement points to the fact that the resulting magnetospheric energization as a result of the electric field becomes more effective for magnetic storm occurrence. The very-intense storm empirical relationship between B and V (0.439) may likely be due to the Corona mass ejection (CME) release and acceleration mechanism occurring near the Sun. Moreover, B_T seems to be more relevant with B for peak Dst $\leq -250\,\text{nT}$.

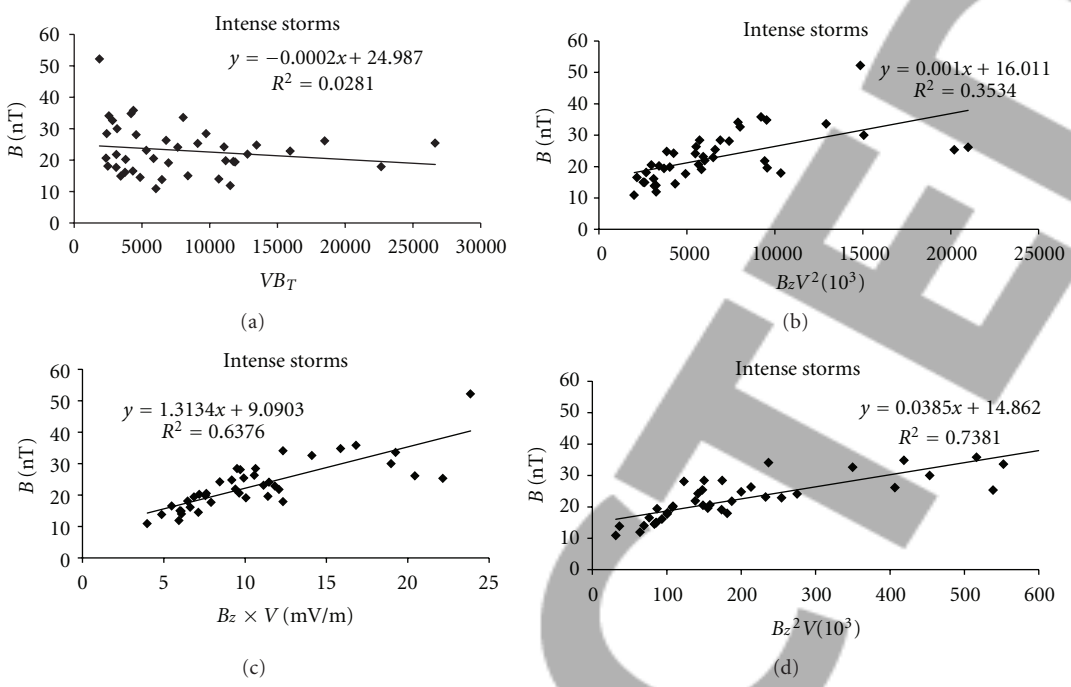

Figure 4: Regression plots of B with some commonly used coupling functions for the Solar Wind-Magnetosphere Interaction (according to [1] and the references therein) for the intense storms under investigation: (a) VB_T, (b) B_zV^2, (c) $B_z \times V$, and (d) $B_{z^2}V$.

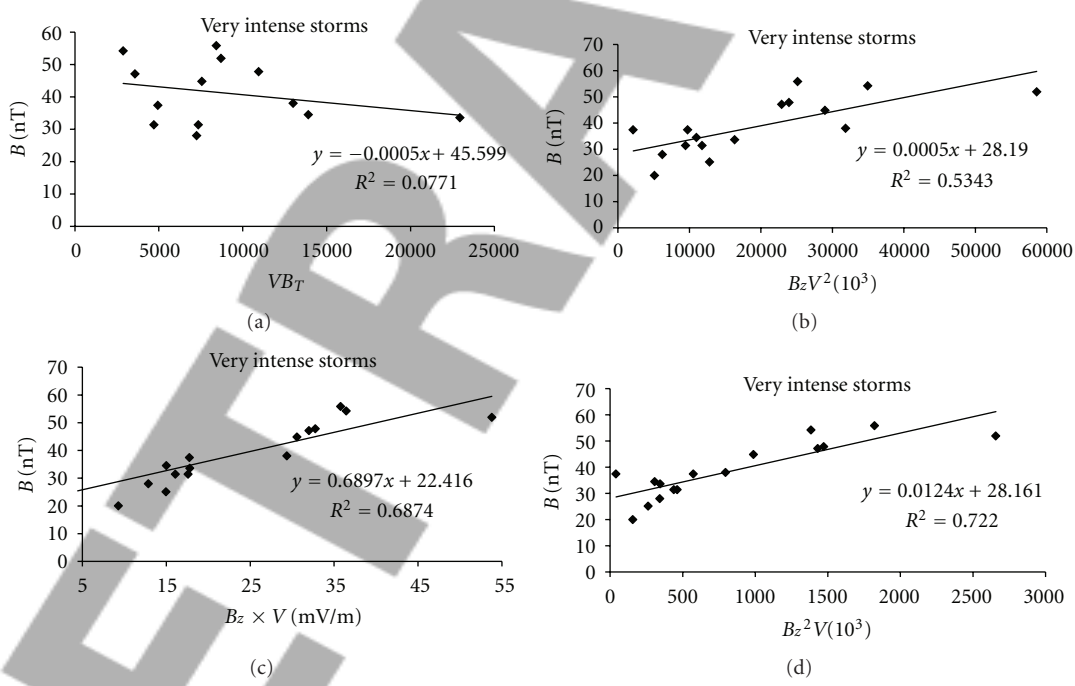

Figure 5: Regression plots of B with some commonly used coupling functions for the Solar Wind-Magnetosphere Interaction for the very intense storms under investigation: (a) VB_T, (b) B_zV^2, (c) $B_z \times V$, and (d) $B_{z^2}V$.

The results from other "indicators" used in the coupling functions for the Solar Wind-Magnetosphere Interaction showed that all the indicators agreed with earlier results, (e.g., [1, 5, 16, 20] and references therein) with a correlation percentage of above 70%. The only exception is the B-VB_T relationship. The strong cross-magnetospheric convection electric fields with associated field-aligned potentials which are also a significance effect of magnetic reconnection and strong magnetic field distortions may be one of the factors responsible for the high correlation value between B and $V \times B_z$ (0.857). The plots in Figure 7 also showed that B_z is the most driving factor for the interplanetary dawn-to-dusk

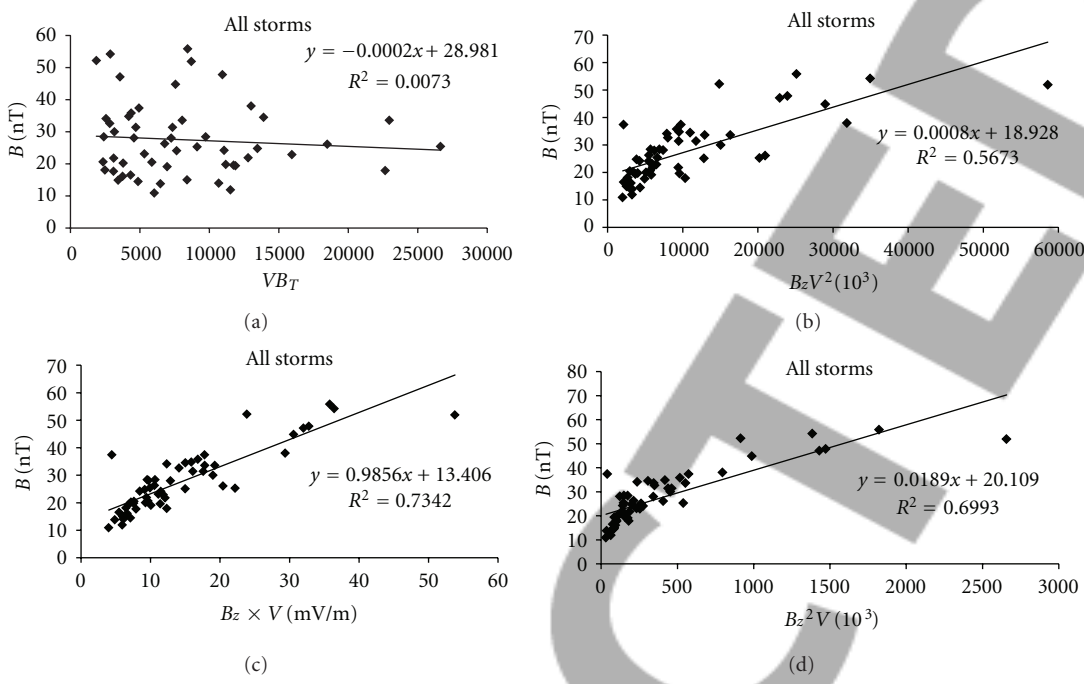

Figure 6: Regression plots of B with some commonly used coupling functions for the Solar Wind-Magnetosphere Interaction for all storms (a) VB_T, (b) B_zV^2, (c) $B_z \times V$, and (d) $B_{z^2}V$.

Table 5: Pearson correlation coefficient between VB_T, B_zV^2, $V \times B_z$, and $B_{z^2}V$ as well as the derived $B_{z^3}V$ and $(V \times B_z)/B_T$ with average magnetic field B.

Nature	B versus VB_T	B versus B_zV^2	B versus $V \times B_z$	B versus $B_{z^2}V$	B versus $B_{z^3}V$	$(V \times B_z)/B_T$
Intense	0.168	0.594	0.798	0.859	0.844	0.761
Very intense	0.278	0.736	0.829	0.850	0.825	0.717
All	0.085	0.753	0.857	0.836	0.801	0.750

electric field. Here, a correlation plot of (a) $V \times B_z$ against B_z gives a value of 0.901, (b) $V \times B_z$ against flow speed V yields 0.709, and (c) V against B_z recorded an apparently low value of 0.391. The result of (b) shows the relevance of the flow speed in the $V \times B_z$ parameter as well but only points to the fact that it is not as geoeffective as B_z as far as generation of intense storms is concerned. The result of (c) implies that both V and B_z are not necessarily dependent of each other, or that their dependency is low. It should be noted that parallel electric fields above the ionosphere may lead to downward acceleration of electrons to energies of 1–10 keV.

The high correlation value of B versus B_z tends to disagree with the work of Adebesin [12], where it was observed that for all storms (i.e., intense and very-intense), the flow speed is the most correlated with B (correlation = 0.509) and hence the most geoeffective, in which case B versus B_z value is as low as 0.219. This can be explained on the following basis. According to Y. I. Yermolaev and M. Y. Yermolaev [21], based on various clarifications, there are six main large-scale types of interplanetary occurrences, namely, (i) fast solar wind from coronal holes, (ii) slow solar wind from coronal streamers, (iii) heliospheric current sheet, (iv) decompressed streams of solar wind, (v) complex ejecta, that is, compressed streams of solar wind (corotating interaction region, CIR, and sheath, streams ahead magnetic clouds, MC), and (vi) magnetic clouds. However, among the six, it is only the last two types that are geoeffctive, just because they can contain long Interplanetary Magnetic Field southward B_z component [22–24]. It is most likely that one or more of the other first four classifications may be the main driver of most of the 18 storms considered by Adebesin [12]. If this is so, then the flow speed will invariably be more correlated with B than with B_z, since it does not involve long southward B_z. Another factor that may contribute to the result may be the limited number of investigated storms (i.e., 18). Another factor may be that most of the storms could have been associated with multiple halo CMEs that may have been intermingling, and such interactions are more likely near maximum and could explain some of the compositional anomalies of ICMEs [25].

From earlier results by different authors, it has been shown that quite a lot of strong magnetic storms (i.e., events of March 31, 2001, Dst peak value of −387 nT; April 11, 2001, Dst = −271 nT [26]; November 20, 2003, Dst = −472 nT [27]; October 29-30, 2003, Dst = −363 nT [28]; November 8–10, 2004, Dst = −373 nT [29]) have been generated as a result of multiple interacting magnetic clouds. However, according to Farrugia et al. [30], it was observed that a significant number of our large events (6 out of 16) consisted of

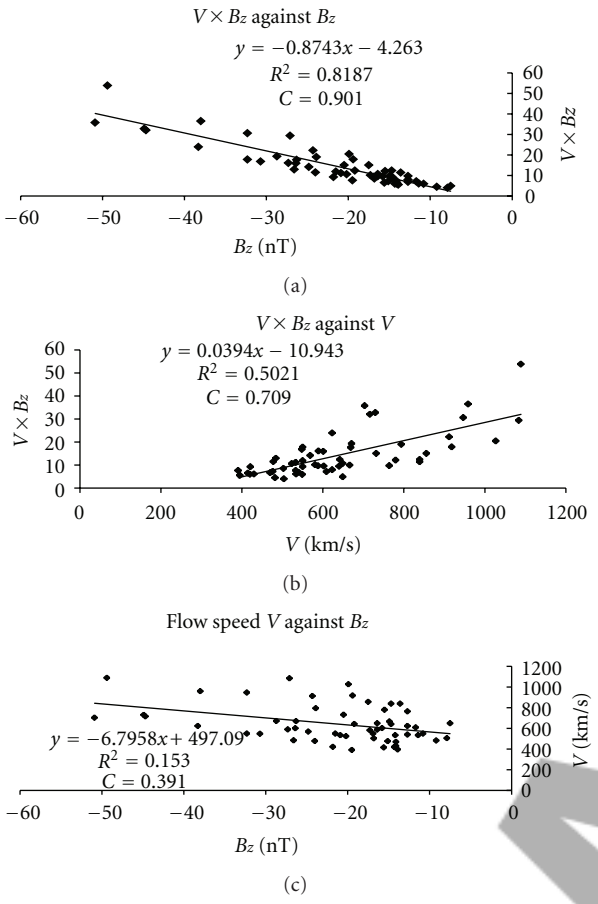

Figure 7: Correlation plots of (a) $V \times B_z$, against B_z. (b) $V \times B_z$ against flow speed V, and (c) V against B_z.

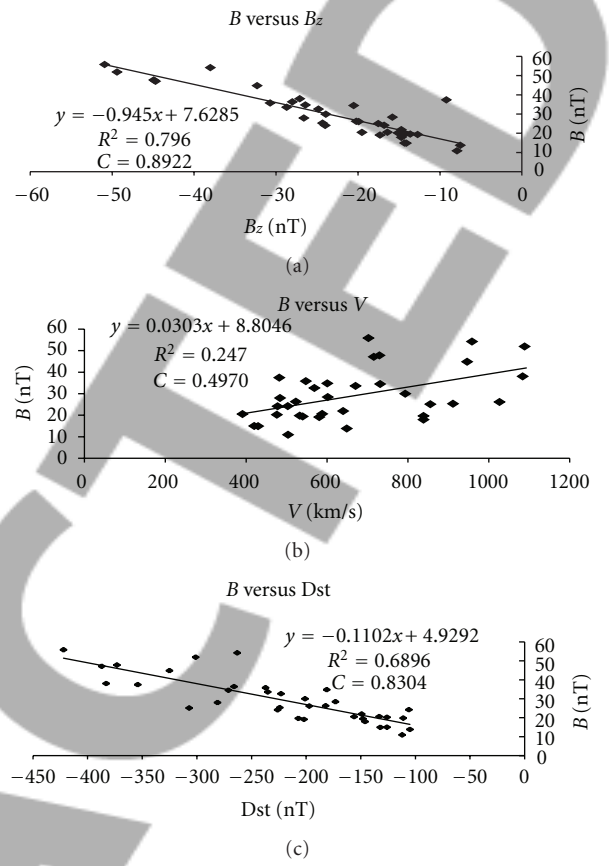

Figure 8: Correlation plots of magnetic field B with (a) B_z, (b) V, and (c) Dst for magnetic cloud events.

Table 6: Summary of the results of Figures 8 and 9 for magnetic cloud and complex ejecta.

	Magnetic cloud	Complex ejecta
Number(out of 58)	36	22
%	62	38
B versus B_z corr.	0.8922	0.7608
B versus V corr.	0.4970	0.2853
B versus Dst corr.	0.8304	0.1105

ICMEs/magnetic clouds interacting with each other forming complex ejecta. In like manner, Xie et al. [31] studied 37 long-lived geomagnetic storms with Dst < -100 nT and the associated CMEs which occurred between 1998 and 2002 and found that 24 of 37 events (∼65%) were caused by successive CMEs and number of interacting magnetic clouds was observed from 2 up to 4.

In light of the above, we went further to investigate for the percentage of storms generated by either the magnetic cloud or complex ejecta. Figures 8 and 9 revealed the correlation plots of Magnetic field B with (a) B_z, (b) V, and (c) Dst for magnetic cloud and complex ejecta events, respectively. It was observed from Figure 8 that there are better plotted points for (a) and (c), while that of (b) was dispersed. Figure 9 also revealed a dispersed plot for (b) and (c). However, the summary of the results was highlighted in Table 6. 62% of the events were as a result of magnetic cloud (MC), while 38% were generated by complex ejecta. The B-B_z relation attained a correlation coefficient of 0.8922, a little above B versus Dst (0.8304), while B-V recorded 0.4970. For the complex ejecta, the B versus B_z correlation is 0.7608. The values are presumably low for the other two parameters. The overall respective high correlation values of the parameters with B during magnetic cloud events over the complex ejecta events seem to suggest that though both classes can cause intense storm, but the former is more geoeffective than the latter.

The frequency distribution of B_T (i.e., the southward B_z duration) for all the storms showed that 41.5% is in the range 3–9 hours, 35.8% (10–19 hours), 18.9% (20–29 hours), and 3.8% (≥30 hours). This shows that about 58.5% of B_T extended beyond 10 hours of southward B_z orientation. The implication of this is that with every southward field turning, there is a decrease in Dst; so the longer the B_T is, the longer is the storm recovery phase (since only northward orientation of the interplanetary magnetic field would aid the recovery phase in most cases). The southward field turnings therefore cause magnetic reconnection and plasma injections into the nightside magnetosphere. However, these periods of continuous substorm activity are known as "high-intensity, long

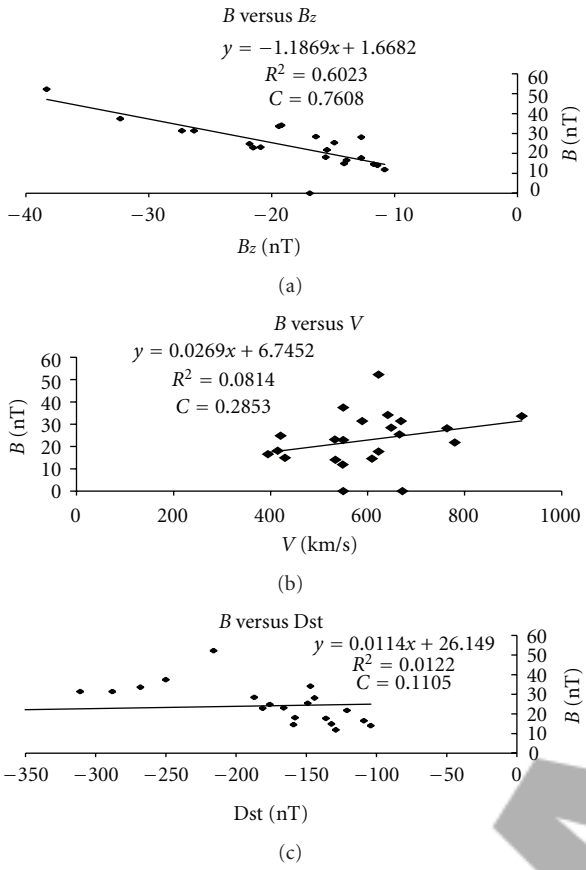

Figure 9: Correlation plots of magnetic field B with (a) B_z, (b) V, and (c) Dst for complex ejecta events.

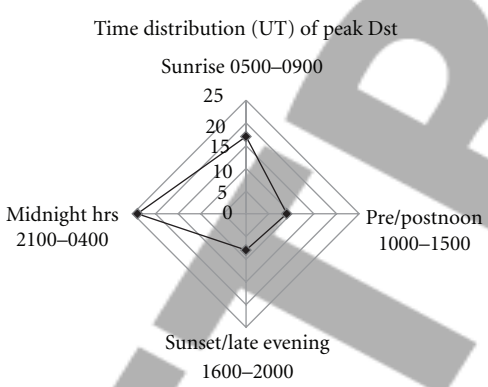

Figure 10: Radial time distribution of peak Dst value for all storms.

duration, continuous AE activities (HILDCAA)". Therefore, the sporadic injection of plasma into the magnetosphere is the reason why the ring current does not appear to decay. However the interplanetary field B_z fluctuations are as a result of Alfven waves present in the high-speed streams when the waves are compressed, leading, in most cases, to irregular shaped storm main phase. This may be responsible for the highest correlation value observed (0.885) for the B-B_z relationship.

According to Gonzalez and Tsurutani [2] and Gosling et al. [3], 90% of storms with intensities of peak Dst ≤ -100 nT

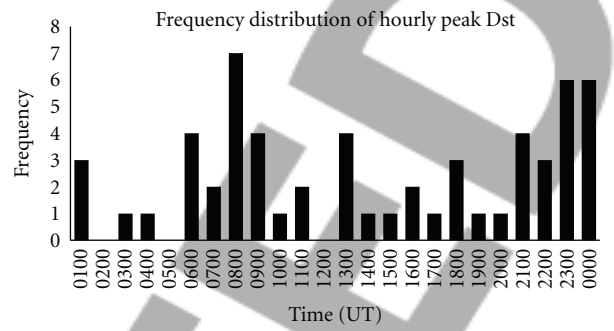

Figure 11: Hourly frequency distribution of peak Dst value for all storms.

are caused by southward magnetic fields within high-speed streams led by shocks.

Figure 10 illustrates the radial time distribution of peak Dst value (i.e., the exact hour of the day that Dst reaches its peak value) for all the 58 storms under investigation. The time was divided into four categories, namely, sunrise (0500–0900 UT), prenoon/postnoon (1000–1500 UT), sunset/late evening (1600–2000 UT), and midnight hours (2100–0400 UT). The figure revealed a 41.2% occurrence for midnight hours, followed by sunrise period with 29.3%. The prenoon/postnoon and the sunset episodes recorded 15.5% and 13.8%, respectively. Moreover, the hourly frequency distribution of peak Dst values was depicted in Figure 11. The figure revealed that the 0800 UT, 2300 UT and 0000 UT recorded the observed highest values. The explanation for this is still left open.

5. Summary and Conclusion

58 storms of different intensities were considered in this study. Previous works have shown that the southward interplanetary magnetic field B_z is the most geoeffective factor in the solar wind-magnetosphere coupling function. However, the result of Adebesin [12] in which 18 storms were observed arrived at the conclusion that the flow speed is the most geoeffective. However, the result of the present study revealed the following.

(i) B_z shows to be more relevant with the magnetic field B for all storms.

(ii) The southward B_z duration B_T seems to be more relevant with B for Dst < -250 nT (i.e., very intense storms).

(iii) Both the V and B_z factors in the interplanetary dawn-dusk electric field ($V \times B_z$) which causes magnetosphere energization are effective in the occurrence of "very intense" storms while "intense" storms are mostly enhanced by the B_z factor alone.

(iv) B_T determines the duration of the recovery phase of the storm.

(v) V and B_z have little or no dependence on each other.

(vi) In contrast to Adebesin [12], B has high correlation with B_z.

(vii) The disagreement with the result of Adebesin [12] was suggested to be due to differences in the causative factors of the storms studied then, and those for the present study, as well as the number of storms considered.

(viii) Observations on the coupling functions for the Solar Wind-Magnetosphere interaction parameters agree with earlier results with regards to $B_z V^2$, $B_z \times V$, and $B_{z^2} V$, as well as the derived ones (i.e., VB_T, $B_{z^3} V$, and $(V \times B_z)/B_T VB_T$).

(ix) Most of the storms were observed to occur at midnight hours, having a 41.2% incidence rate, followed by the sunrise hours (with 29.3%).

(x) 62% of the events were as a result of magnetic cloud (MC), while 38% were generated by complex ejecta. The B-B_z relation for the magnetic cloud attained a correlation coefficient of 0.8922. For the complex ejecta, the B versus B_z correlation is 0.7608.

We therefore can say from the above that the B_z factor in the $(V \times B_z)$ parameter (i.e., the interplanetary dawn-dusk electric field) is very geoeffective for both the $-250\,\text{nT} \leq$ peak Dst < -100 nT and peak Dst < -250 nT class of storms, whereas the flow speed V is only effective for the first class alone (in most cases).

Acknowledgment

The author would like to thank NSSDC's OMNI database (http://nssdc.gsfc.nasa.gov/omniweb/) for their data support.

References

[1] W. D. Gonzalez, J. A. Joselyn, Y. Kamide et al., "What is a geomagnetic storm?" *Journal of Geophysical Research*, vol. A4, pp. 5771–5792, 1994.

[2] W. D. Gonzalez and B. T. Tsurutani, "Criteria of interplanetary parameters causing intense magnetic storms," *Planetary and Space Science*, vol. 35, no. 9, pp. 1101–1109, 1987.

[3] J. T. Gosling, D. J. McComas, J. L. Phillips, and S. J. Bame, "Geomagnetic activity associated with earth passage of interplanetary shock disturbances and coronal mass ejections," *Journal of Geophysical Research*, vol. 69, pp. 7831–7839, 1991.

[4] G. Lu, T. E. Holzer, D. Lummerzheim et al., "Ionospheric response to the interplanetary magnetic field southward turning: fast onset and slow reconfiguration," *Journal of Geophysical Research A: Space Physics*, vol. 107, no. 8, pp. 1153–1159, 2002.

[5] W. D. Gonzalez, A. L. Clua de Gonzalez, J. H. A. Sobral, and L. E. Vieira, "Solar and Interplanetry causes of very intense storms," *Journal of Atmospheric and Terrestrial Physics*, vol. 63, pp. 403–412, 2001.

[6] G. Rostoker, L. Lam, and W. D. Hume, "Response time of the magnetosphere to the interplanetary electric field," *Canadian Journal of Physics*, vol. 50, p. 544, 1972.

[7] R. K. Burton, R. L. McPherron, and C. T. Russell, "An empirical relationship between interplanetary conditions and Dst," *Journal of Geophysical Research*, vol. 80, article 4204, 1975.

[8] R. L. Arnoldy, "Signature in interplanetary medium for substorms," *Journal of Geophysical Research*, vol. 76, p. 5189, 1971.

[9] B. T. Tsurutani and C. I. Meng, "Interplanetary magnetic field variations and substorm activity," *Journal of Geophysical Research*, vol. 77, p. 2964, 1972.

[10] R. E. Holzer and J. A. Slavin, "An evaluation of three predictors of geomagnetic activity," *Journal of Geophysical Research*, vol. 87, p. 2558, 1982.

[11] D. N. Baker, R. D. Zwickl, S. J. Bame et al., "Isee 3 high time resolution study of interplanetary parameter correlations with magnetospheric activity," *Journal of Geophysical Research*, vol. 88, no. 8, pp. 6230–6242, 1983.

[12] B. O. Adebesin, "Roles of interplanetary and geomagnetic parameters in "intense" and "very intense" magnetic storms generation and their geoeffectiveness," *Acta Geodaetica et Geophysica Hungarica*, vol. 43, no. 4, pp. 383–408, 2008.

[13] J. R. Taylor, M. Lester, and T. K. Yeoman, "A superposed epoch analysis of geomagnetic storms," *Annals of Geophysics*, vol. 12, p. 612, 1994.

[14] B. T. Tsurutani, W. D. Gonzalez, F. Tang, S.-I. Akasofu, and E. J. Smith, "Origin of Interplanetary southward magnetic storms near solar maximum (1978–1979)," *Journal of Geophysical Research*, vol. 93, p. 8519, 1988.

[15] A. Dal Lago, L. E. A. Vieira, E. Echer et al., "Great geomagnetic storms in the rise and maximum of solar cycle 23," *Brazilian Journal of Physics*, vol. 34, no. 4B, pp. 1542–1546, 2004.

[16] P. Ballatore, "Effects of fast and slow solar wind on the correlations between interplanetary medium and geomagnetic activity," *Journal of Geophysical Research A: Space Physics*, vol. 107, article 1227, 2002.

[17] C. A. Loewe and G. W. Prolss, "Classification and mean behavior of magnetic storms," *Journal of Geophysical Research A: Space Physics*, vol. 102, no. 7, pp. 14209–14213, 1997.

[18] C. Y. Huang, W. J. Burke, and C. S. Lin, "Ion precipitation in the dawn sector during geomagnetic storms," *Journal of Geophysical Research A: Space Physics*, vol. 110, no. 11, Article ID A11213, 2005.

[19] L. E. A. Vieira, W. D. Gonzalez, A. J. Clua de Gonzalez, and A. Dal Lago, "A study of magnetic Storms development in two or more steps and its association with the polarity of magnetic cloud," *Journal of Atmospheric and Solar-Terrestrial Physics*, vol. 63, no. 5, pp. 457–461, 2000.

[20] T. I. Pulkkinen, N. Partamies, K. E. J. Huttunen, G. D. Reeves, and H. E. J. Koskinen, "Differences in geomagnetic storms driven by magnetic clouds and ICME sheath regions," *Geophysical Research Letters*, vol. 34, no. 2, Article ID L02105, 2007.

[21] Y. I. Yermolaev and M. Y. Yermolaev, "Statistic study on the geomagnetic storm effectiveness of solar and interplanetary events," *Advances in Space Research*, vol. 37, no. 6, pp. 1175–1181, 2006.

[22] J. T. Gosling and V. J. Pizzo, "Formation and evolution of corotating interaction regions and their three dimensional structure," *Space Science Reviews*, vol. 89, no. 1-2, pp. 21–25, 1999.

[23] W. D. Gonzalez, B. T. Tsurutani, and A. L. Clúa de Gonzalez, "Interplanetary origin of geomagnetic storms," *Space Science Reviews*, vol. 88, no. 3-4, pp. 529–562, 1999.

[24] V. Bothmer, "The solar and interplanetary causes of space storms in solar cycle 23," *IEEE Transactions on Plasma Science*, vol. 32, no. 4 I, pp. 1411–1414, 2004.

[25] N. Gopalswamy, S. Yashiro, M. L. Kaiser, R. A. Howard, and J. L. Bougeret, "Radio signatures of coronal mass ejection

interaction: coronal mass ejection cannibalism?" *Astrophysical Journal*, vol. 548, no. 1, pp. L91–L94, 2001.

[26] Y. M. Wang, P. Z. Ye, and S. Wang, "Multiple magnetic clouds: several 21examples during March-April 2001," *Journal of Geophysical Research*, vol. 108, no. A10, p. 1370, 2003.

[27] N. Gopalswamy, S. Yashiro, G. Michalek, H. Xie, R. P. Lepping, and R. A. Howard, "Solar source of the largest geomagnetic storm of cycle 23," *Geophysical Research Letters*, vol. 32, no. 12, pp. 1–5, 2005.

[28] I. S. Veselovsky, M. I. Panasyuk, S. I. Avdyushin et al., "Solar and heliospheric phenomena in October-November 2003: causes and consequences," *Kosmicheskie Issledovaniia*, vol. 42, no. 5, p. 453, 2004 (Russian).

[29] Y. I. Yermolaev, L. M. Zelenyi, G. N. Zastenker et al., "A year later: solar, heliospheric, and magnetospheric disturbances in November 2004," *Geomagnetism and Aeronomy*, vol. 45, no. 6, pp. 681–719, 2005.

[30] C. J. Farrugia, H. Matsui, H. Kucharek et al., "Survey of intense Sun-Earth connection events (1995–2003)," *Advances in Space Research*, vol. 38, no. 3, pp. 498–502, 2006.

[31] H. Xie, N. Gopalswamy, P. K. Manoharan, A. Lara, S. Yashiro, and S. Lepri, "Long-lived geomagnetic storms and coronal mass ejections," *Journal of Geophysical Research A: Space Physics*, vol. 111, no. 1, Article ID A01103, 2006.